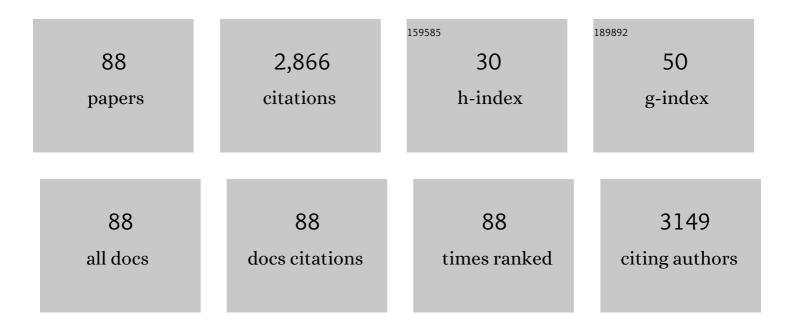
List of Publications by Year in descending order

Source: https://exaly.com/author-pdf/5686623/publications.pdf Version: 2024-02-01



KVIE D OLINN

| # | Article | IF | CITATIONS |
|----|--|------|-----------|
| 1 | Optical Imaging Using Endogenous Contrast to Assess Metabolic State. Annual Review of Biomedical Engineering, 2012, 14, 351-367. | 12.3 | 257 |
| 2 | Quantitative metabolic imaging using endogenous fluorescence to detect stem cell differentiation. Scientific Reports, 2013, 3, 3432. | 3.3 | 215 |
| 3 | Evaluating Cell Metabolism Through Autofluorescence Imaging of NAD(P)H and FAD. Antioxidants and Redox Signaling, 2019, 30, 875-889. | 5.4 | 171 |
| 4 | Young developmental age cardiac extracellular matrix promotes the expansion of neonatal cardiomyocytes in vitro. Acta Biomaterialia, 2014, 10, 194-204. | 8.3 | 168 |
| 5 | Endogenous Two-Photon Fluorescence Imaging Elucidates Metabolic Changes Related to Enhanced Glycolysis and Glutamine Consumption in Precancerous Epithelial Tissues. Cancer Research, 2014, 74, 3067-3075. | 0.9 | 129 |
| 6 | Mapping metabolic changes by noninvasive, multiparametric, high-resolution imaging using endogenous contrast. Science Advances, 2018, 4, eaap9302. | 10.3 | 128 |
| 7 | Skin Structure–Function Relationships and the Wound Healing Response to Intrinsic Aging. Advances in Wound Care, 2020, 9, 127-143. | 5.1 | 87 |
| 8 | Imaging mitochondrial dynamics in human skin reveals depth-dependent hypoxia and malignant potential for diagnosis. Science Translational Medicine, 2016, 8, 367ra169. | 12.4 | 82 |
| 9 | Characterization of metabolic changes associated with the functional development of 3D engineered tissues by non-invasive, dynamic measurement of individual cell redox ratios. Biomaterials, 2012, 33, 5341-5348. | 11.4 | 77 |
| 10 | Optical redox ratio identifies metastatic potential-dependent changes in breast cancer cell metabolism. Biomedical Optics Express, 2016, 7, 4364. | 2.9 | 76 |
| 11 | Altered collagen fiber kinematics define the onset of localized ligament damage during loading. Journal of Applied Physiology, 2008, 105, 1881-1888. | 2.5 | 65 |
| 12 | Neuronal hyperexcitability in the dorsal horn after painful facet joint injury. Pain, 2010, 151, 414-421. | 4.2 | 62 |
| 13 | Cervical facet capsular ligament yield defines the threshold for injury and persistent joint-mediated neck pain. Journal of Biomechanics, 2007, 40, 2299-2306. | 2.1 | 60 |
| 14 | Glutamine Metabolism Controls Stem Cell Fate Reversibility and Long-Term Maintenance in the Hair Follicle. Cell Metabolism, 2020, 32, 629-642.e8. | 16.2 | 60 |
| 15 | In vivo multiphoton microscopy detects longitudinal metabolic changes associated with delayed skin wound healing. Communications Biology, 2018, 1, 198. | 4.4 | 58 |
| 16 | Automated quantification of three-dimensional organization of fiber-like structures in biological tissues. Biomaterials, 2017, 116, 34-47. | 11.4 | 55 |
| 17 | Rapid quantification of pixel-wise fiber orientation data in micrographs. Journal of Biomedical Optics, 2013, 18, 046003. | 2.6 | 53 |
| 18 | Rapid three-dimensional quantification of voxel-wise collagen fiber orientation. Biomedical Optics Express, 2015, 6, 2294. | 2.9 | 52 |

| # | Article | IF | CITATIONS |
|----|---|------|-----------|
| 19 | Preconditioning is Correlated With Altered Collagen Fiber Alignment in Ligament. Journal of Biomechanical Engineering, 2011, 133, 064506. | 1.3 | 51 |
| 20 | Skin Rejuvenation with Non-Invasive Pulsed Electric Fields. Scientific Reports, 2015, 5, 10187. | 3.3 | 45 |
| 21 | From Single Cells to Tissues: Interactions between the Matrix and Human Breast Cells in Real Time. PLoS ONE, 2014, 9, e93325. | 2.5 | 39 |
| 22 | Noninvasive Metabolic Imaging of Engineered 3D Human Adipose Tissue in a Perfusion Bioreactor. PLoS ONE, 2013, 8, e55696. | 2.5 | 38 |
| 23 | Improved Fourier-based characterization of intracellular fractal features. Optics Express, 2012, 20, 23442. | 3.4 | 37 |
| 24 | Noninvasive assessment of mitochondrial organization in three-dimensional tissues reveals changes associated with cancer development. International Journal of Cancer, 2015, 136, 322-332. | 5.1 | 36 |
| 25 | Non-invasive monitoring of cell metabolism and lipid production in 3D engineered human adipose tissues using label-free multiphoton microscopy. Biomaterials, 2013, 34, 8607-8616. | 11.4 | 35 |
| 26 | Optical metrics of the extracellular matrix predict compositional and mechanical changes after myocardial infarction. Scientific Reports, 2016, 6, 35823. | 3.3 | 35 |
| 27 | Vector correlation technique for pixel-wise detection of collagen fiber realignment during injurious tensile loading. Journal of Biomedical Optics, 2009, 14, 054010. | 2.6 | 34 |
| 28 | An automated image processing method to quantify collagen fibre organization within cutaneous scar tissue. Experimental Dermatology, 2015, 24, 78-80. | 2.9 | 34 |
| 29 | Quantitative characterization of mineralized silk film remodeling during long-term osteoblast–osteoclast co-culture. Biomaterials, 2014, 35, 3794-3802. | 11.4 | 33 |
| 30 | Structural changes in the cervical facet capsular ligament: potential contributions to pain following subfailure loading. Stapp Car Crash Journal, 2007, 51, 169-87. | 1.1 | 33 |
| 31 | Valve interstitial cell contractile strength and metabolic state are dependent on its shape. Integrative Biology (United Kingdom), 2016, 8, 1079-1089. | 1.3 | 32 |
| 32 | Endogenous Two-Photon Excited Fluorescence Imaging Characterizes Neuron and Astrocyte Metabolic Responses to Manganese Toxicity. Scientific Reports, 2017, 7, 1041. | 3.3 | 32 |
| 33 | Anomalous fiber realignment during tensile loading of the rat facet capsular ligament identifies mechanically induced damage and physiological dysfunction. Journal of Biomechanics, 2010, 43, 1870-1875. | 2.1 | 30 |
| 34 | Diabetic Wounds Exhibit Distinct Microstructural and Metabolic Heterogeneity through Label-Free Multiphoton Microscopy. Journal of Investigative Dermatology, 2016, 136, 342-344. | 0.7 | 29 |
| 35 | Non-destructive two-photon excited fluorescence imaging identifies early nodules in calcific aortic-valve disease. Nature Biomedical Engineering, 2017, 1, 914-924. | 22.5 | 29 |
| 36 | 3D organizational mapping of collagen fibers elucidates matrix remodeling in a hormone-sensitive 3D breast tissue model. Biomaterials, 2018, 179, 96-108. | 11.4 | 28 |

| # | Article | IF | CITATIONS |
|----|---|------|-----------|
| 37 | Head-Turned Postures Increase the Risk of Cervical Facet Capsule Injury During Whiplash. Spine, 2008, 33, 1643-1649. | 2.0 | 27 |
| 38 | Full field strain measurements of collagenous tissue by tracking fiber alignment through vector correlation. Journal of Biomechanics, 2010, 43, 2637-2640. | 2.1 | 24 |
| 39 | Hormonal Regulation of Epithelial Organization in a Three-Dimensional Breast Tissue Culture Model. Tissue Engineering - Part C: Methods, 2014, 20, 42-51. | 2.1 | 23 |
| 40 | Detection of Altered Collagen Fiber Alignment in the Cervical Facet Capsule After Whiplash-Like Joint Retraction. Annals of Biomedical Engineering, 2011, 39, 2163-2173. | 2.5 | 22 |
| 41 | Preventing Scars after Injury with Partial Irreversible Electroporation. Journal of Investigative Dermatology, 2016, 136, 2297-2304. | 0.7 | 22 |
| 42 | Skin regeneration with all accessory organs following ablation with irreversible electroporation. Journal of Tissue Engineering and Regenerative Medicine, 2018, 12, 98-113. | 2.7 | 22 |
| 43 | Characterizing differences in the collagen fiber organization of skin wounds using quantitative polarized light imaging. Wound Repair and Regeneration, 2019, 27, 711-714. | 3.0 | 22 |
| 44 | Cellâ€Tethered Ligands Modulate Bone Remodeling by Osteoblasts and Osteoclasts. Advanced Functional Materials, 2014, 24, 472-479. | 14.9 | 21 |
| 45 | Optical imaging of radiation-induced metabolic changes in radiation-sensitive and resistant cancer cells. Journal of Biomedical Optics, 2017, 22, 060502. | 2.6 | 19 |
| 46 | A Radiosensitizing Inhibitor of HIF-1 alters the Optical Redox State of Human Lung Cancer Cells In Vitro. Scientific Reports, 2018, 8, 8815. | 3.3 | 18 |
| 47 | The role of graded nerve root compression on axonal damage, neuropeptide changes, and pain-related behaviors. Stapp Car Crash Journal, 2008, 52, 33-58. | 1.1 | 18 |
| 48 | Quantifying Age-Related Changes in Skin Wound Metabolism Using <i>In Vivo</i> Multiphoton Microscopy. Advances in Wound Care, 2020, 9, 90-102. | 5.1 | 17 |
| 49 | Membrane potential depolarization causes alterations in neuron arrangement and connectivity in cocultures. Brain and Behavior, 2015, 5, 24-38. | 2.2 | 15 |
| 50 | Quantitative differentiation of normal and scarred tissues using secondâ€harmonic generation microscopy. Scanning, 2016, 38, 684-693. | 1.5 | 13 |
| 51 | Three-Dimensional Quantification of Collagen Microstructure During Tensile Mechanical Loading of Skin. Frontiers in Bioengineering and Biotechnology, 2021, 9, 642866. | 4.1 | 13 |
| 52 | Equine model for softâ€ŧissue regeneration. Journal of Biomedical Materials Research - Part B Applied Biomaterials, 2015, 103, 1217-1227. | 3.4 | 11 |
| 53 | Rapid quantification of mitochondrial fractal dimension in individual cells. Biomedical Optics Express, 2018, 9, 5269. | 2.9 | 9 |
| 54 | Rejuvenation of aged rat skin with pulsed electric fields. Journal of Tissue Engineering and Regenerative Medicine, 2018, 12, 2309-2318. | 2.7 | 8 |

| # | Article | IF | CITATIONS |
|----|---|--------------|-------------------------------|
| 55 | Biocompatible, Injectable Anionic Hydrogels Based on Poly(Oligo Ethylene Glycol) Tj ETQq1 1 0.784314 rgBT /Ove | rlock 3.2 | 10 Tf <mark>5</mark> 0 742 To |
| 56 | Differences in colonic crypt morphology of spontaneous and colitis-associated murine models via second harmonic generation imaging to quantify colon cancer development. BMC Cancer, 2019, 19, 428. | 2.6 | 7 |
| 57 | Label-free metabolic biomarkers for assessing valve interstitial cell calcific progression. Scientific Reports, 2020, 10, 10317. | 3.3 | 7 |
| 58 | Non-invasive Assessments of Adipose Tissue Metabolism In Vitro. Annals of Biomedical Engineering, 2016, 44, 725-732. | 2.5 | 6 |
| 59 | Automated Extraction of Skin Wound Healing Biomarkers From In Vivo Labelâ€Free Multiphoton Microscopy Using Convolutional Neural Networks. Lasers in Surgery and Medicine, 2021, 53, 1086-1095. | 2.1 | 4 |
| 60 | Efficacy of Combined in-vivo Electroporation-Mediated Gene Transfer of VEGF, HGF, and IL-10 on Skin Flap Survival, Monitored by Label-Free Optical Imaging: A Feasibility Study. Frontiers in Surgery, 2021, 8, 639661. | 1.4 | 4 |
| 61 | Multiscale Computational Model Predicts Mouse Skin Kinematics Under Tensile Loading. Journal of Biomechanical Engineering, 2022, 144, . | 1.3 | 4 |
| 62 | Label-free optical biomarkers detect early calcific aortic valve disease in a wild-type mouse model. BMC Cardiovascular Disorders, 2020, 20, 521. | 1.7 | 3 |
| 63 | Label-Free Multiphoton Microscopy for the Detection and Monitoring of Calcific Aortic Valve Disease. Frontiers in Cardiovascular Medicine, 2021, 8, 688513. | 2.4 | 3 |
| 64 | Single Dose of N-Acetylcysteine in Local Anesthesia Increases Expression of HIF1α, MAPK1, TGFβ1 and Growth Factors in Rat Wound Healing. International Journal of Molecular Sciences, 2021, 22, 8659. | 4.1 | 3 |
| 65 | Autocorrelation method for fractal analysis in nonrectangular image domains. Optics Letters, 2013, 38, 4477. | 3.3 | 2 |
| 66 | N-Acetylcysteine Added to Local Anesthesia Reduces Scar Area and Width in Early Wound Healing—An Animal Model Study. International Journal of Molecular Sciences, 2021, 22, 7549. | 4.1 | 2 |
| 67 | Characterizing diabetic wound metabolism and microstructure using multi-photon microscopy. , 2014, , , \cdot | | 1 |
| 68 | Automated Quantitative Analysis of Wound Histology Using Deep-Learning Neural Networks. Journal of Investigative Dermatology, 2021, 141, 1367-1370. | 0.7 | 1 |
| 69 | Tissue Imaging and Quantification Relying on Endogenous Contrast. Advances in Experimental Medicine and Biology, 2021, 3233, 257-288. | 1.6 | 1 |
| 70 | Functional Imaging of Wound Metabolism. Frontiers in Nanobiomedical Research, 2017, , 201-230. | 0.1 | 1 |
| 71 | Non-invasive Optical Detection of Cell Differentiation Status Using Endogenous Sources of Optical Contrast. , 2012, , . | | Ο |
| 72 | Non-destructive, label-free metabolic mapping during stem cell differentiation. , 2013, , . | | 0 |

Non-destructive, label-free metabolic mapping during stem cell differentiation. , 2013, , . 72

| # | Article | IF | CITATIONS |
|----|--|-----|-----------|
| 73 | Quantitative optical biomarkers for non-invasive detection of cancerous transformation in live, 3D squamous epithelia. , 2014, , . | | 0 |
| 74 | Joint Distractions Sufficient to Produce Pain Increase Collagen Fiber Undulation in the Cervical Facet Capsular Ligament in the Rat. , 2008, , . | | 0 |
| 75 | The Onset of Structural Yield During Tensile Loading Increases With Age in the Pediatric PMHS Cervical Spine. , 2009, , . | | 0 |
| 76 | Force at Damage and Failure Decreases With Age in the Human Cadaveric Facet Capsular Ligament During Tension. , 2009, , . | | 0 |
| 77 | Microstructural Modeling of Fiber Kinematics and Biomechanics of the Human Facet Capsular Ligament During Subfailure Loading. , 2010, , . | | 0 |
| 78 | Localizing Damage in the Cervical Facet Capsular Ligament With Image-Based Multiscale Models. , 2010, , . | | 0 |
| 79 | Imaging Approaches to Quantify Tissue Structure and Function from the Microscale to the Macroscale. , 2012, , 485-512. | | 0 |
| 80 | Quantitative, Functional Biomarkers of Stem Cell Differentiation in 3D Using Multi-modal Non-linear Imaging with Endogenous Contrast. , 2013, , . | | 0 |
| 81 | Monitoring Osteoblastic Differentiation with Multivariate Analysis of Fluorescence Lifetime Imaging. , 2013, , . | | 0 |
| 82 | Rapid quantification of pixel-wise fiber orientation data in micrographs. Journal of Biomedical Optics, 2013, 18, 040102. | 2.6 | 0 |
| 83 | Label-free assessment of mitochondrial organization in three-dimensional tissues. , 2014, , . | | 0 |
| 84 | Non-linear optical characterization of extracellular matrix changes following myocardial infarction. , 2015, , . | | 0 |
| 85 | In vivo label-free multiphoton microscopy for monitoring delayed skin wound healing. , 2019, , . | | 0 |
| 86 | Quantifying 3D tissue kinematics though second harmonic generation microscopy of skin during mechanical loading. , 2021, , . | | 0 |
| 87 | Optical Imaging of Metabolic Changes in Human Lung Tumor-Adjacent Normal Tissue. , 2020, , . | | 0 |
| 88 | Segmenting Cutaneous Wounds from Tissue Sections and In Vivo Images using Deep Learning. , 2020, , . | | 0 |